Eur. Phys. J. B (2012) 85: 176
DOI: 10.1140/epjb/e2012-21038-y

THE EUROPEAN PHYSICAL JOURNAL B

Regular Article

Trapped modes in finite quantum waveguides

A.L. Delitsyn[1], B.T. Nguyen[2], and D.S. Grebenkov[2,3,4,a]

[1] Mathematical Department of the Faculty of Physics, Moscow State University, 119991 Moscow, Russia
[2] Laboratoire de Physique de la Matière Condensée (UMR 7643), CNRS – Ecole Polytechnique, 91128 Palaiseau, France
[3] Laboratoire Poncelet (UMI 2615), CNRS – Independent University of Moscow, Bolshoy Vlasyevskiy Pereulok 11, 119002 Moscow, Russia
[4] Chebyshev Laboratory, Saint Petersburg State University, 14th line of Vasil'evskiy Ostrov 29, Saint Petersburg, Russia

Received 16 December 2011 / Received in final form 29 February 2012
Published online 30 May 2012 –

Abstract. The eigenstates of an electron in an infinite quantum waveguide (e.g., a bent strip or a twisted tube) are often trapped or localized in a bounded region that prohibits the electron transmission through the waveguide at the corresponding energies. We revisit this statement for resonators with long but finite branches that we call "finite waveguides". Although the Laplace operator in bounded domains has no continuous spectrum and all eigenfunctions have finite L_2 norm, the trapping of an eigenfunction can be understood as its exponential decay inside the branches. We describe a general variational formalism for detecting trapped modes in such resonators. For finite waveguides with general cylindrical branches, we obtain a sufficient condition which determines the minimal length of branches for getting a trapped eigenmode. Varying the branch lengths may switch certain eigenmodes from non-trapped to trapped or, equivalently, the waveguide state from conducting to insulating. These concepts are illustrated for several typical waveguides (L-shape, bent strip, crossing of two strips, etc.). We conclude that the well-established theory of trapping in infinite waveguides may be incomplete and require further development for applications to finite-size microscopic quantum devices.

1 Introduction

The theory of quantum waveguides has been often employed to describe and model microelectronic devices [1–6]. In a high purity crystallic semiconductor, the electron mean free path can be orders of magnitude larger than the size of the structure that allows one to consider the electron as a free particle [7]. In this approximation, the original many-body Schrödinger equation is replaced by the Helmholtz equation with Dirichlet boundary condition. The latter mathematical problem also describes the electromagnetic waves in microwave and optical waveguides [8]. The transmission properties of a waveguide are characterized by its resonance frequencies, i.e. by the spectrum of the Laplace operator. In general, the Laplacian spectrum consists in two parts: (i) the discrete (or point-like) spectrum, with eigenfunctions of finite L_2 norm that are necessarily "trapped" or "localized" in a bounded region of the waveguide; and (ii) the continuous spectrum, with associated functions of infinite L_2 norm that are extended over the whole domain. The continuous spectrum may also contain embedded eigenvalues whose eigenfunctions have finite L_2 norm. A wave excited at the frequency of a trapped eigenmode remains in the bounded region and does not propagate. Similarly, an electron at the energy of a trapped eigenmode does not move through the quantum waveguide, strongly reducing its conductivity. Since the presence of such eigenmodes drastically changes the transmission properties of waveguides, their qualitative understanding and quantitative characterization are important for describing microelectronic, microwave and optical devices.

The existence of trapped, bound or localized eigenmodes in classical and quantum waveguides has been thoroughly investigated in mathematical and applied physics (see [6], reviews [7,9] and also references in [10]). In the seminal paper, Rellich proved the existence of a localized eigenfunction in a deformed infinite cylinder [11]. His results were significantly extended by Jones [12]. Ursell reported on the existence of trapped modes in surface water waves in channels [13–15], while Parker observed experimentally the trapped modes in locally perturbed acoustic waveguides [16,17]. Exner and Seba considered an infinite bent strip of smooth curvature and showed the existence of trapped modes by reducing the problem to Schrödinger operator in the straight strip, with the potential depending on the curvature [18]. Goldstone and Jaffe gave the variational proof that the wave equation subject to Dirichlet boundary condition always has a localized eigenmode in an infinite tube of constant cross-section

[a] e-mail: denis.grebenkov@polytechnique.edu

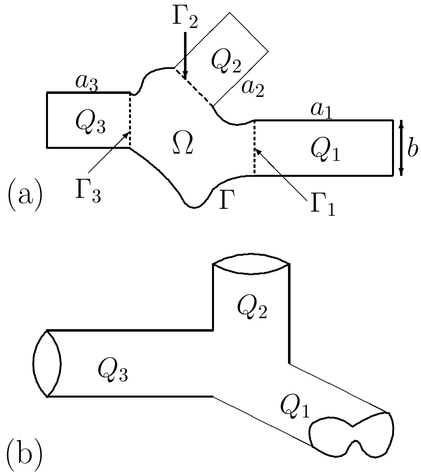

Fig. 1. Two examples of a finite waveguide: (a) a planar bounded domain D which is composed of a basic domain Ω of arbitrary shape and three rectangular branches Q_i of lengths a_i and width b; (b) a three-dimensional bounded domain with three general cylindrical branches.

in two and three dimensions, provided that the tube is not exactly straight [19]. This result was further extended by Chenaud et al. to arbitrary dimension [20]. The problem of localization in acoustic waveguides with Neumann boundary condition has also been investigated [21,22]. For instance, Evans et al. considered a straight strip with an inclusion of arbitrary (but symmetric) shape [22] (see [23] for further extension). Such an inclusion obstructed the propagation of waves and was shown to result in trapped modes. The effect of mixed Dirichlet, Neumann and Robin boundary conditions on the localization was also investigated (see [10,24–26] and references therein). A mathematical analysis of guided water waves was developed in [27]. Lower bounds for the eigenvalues below the cut-off frequency (for which the associated eigenfunctions are localized) were obtained by Ashbaugh and Exner for infinite thin tubes in two and three dimensions [28]. In addition, these authors derived an upper bound for the number of the trapped modes. More recently, Exner et al. considered the Laplacian in finite-length curved tubes of arbitrary cross-section, subject to Dirichlet boundary conditions on the cylindrical surface and Neumann conditions at the ends of the tube. They expressed a lower bound for the spectral threshold of the Laplacian through the lowest eigenvalue of the Dirichlet Laplacian in a torus determined by the geometry of the tube [29].

All the aforementioned works (except the last one) dealt with infinite waveguides for which the Laplace operator spectrum is continuous, with a possible inclusion of isolated or embedded eigenvalues. Since they were responsible for trapped modes, the major question was whether or not such eigenvalues exist. It is worth noting that the localized modes have to decay relatively fast at infinity in order to guarantee the finite L_2 norm. But the same question about the existence of rapidly decaying eigenfunctions may be formulated for bounded domains (resonators) with long branches that we call “finite waveguides” (Fig. 1). This problem is different in many aspects. Since all eigenfunctions have now finite L_2 norms, the definition of trapped or localized modes has to be revised. Quite surprisingly, a rigorous definition of localization in bounded domains turns out to be a challenging problem [30–32]. In the context of the present paper concerning finite waveguides, an eigenmode is called trapped or localized if it decays exponentially fast in prominent subregions (branches) of a bounded domain. A sufficient condition for the exponential decay of an eigenfunction along the branch can be related to the smallness of the associated eigenvalue in comparison to the cut-off frequency, i.e. the first eigenvalue of the Laplace operator in the cross-section of that branch [8]. In other words, the existence of a trapped mode is related to “smallness” of the eigenvalue, in full analogy to infinite waveguides (here, we focus on isolated eigenvalues below the continuous spectrum; note that the eigenfunctions associated to embedded eigenvalues may also decay exponentially). Using the standard mathematical tools such as domain decomposition, explicit representation of solutions of the Helmholtz equation and variational principle, we aim at formalizing these ideas and providing a sufficient condition on the branch lengths for getting a trapped mode. The dependence of the localization character (i.e., the conductivity) on the length of branches is the main result of the paper and a new feature of finite waveguides which was overseen in the well-established theory of infinite waveguides. It is worth recalling that a physical justification for considering infinite quantum waveguides relied on the fact that their length was typically several orders of magnitude bigger than their width [7]. The recent progress in lithography led to further miniaturization of microelectronic devices for which an approximation by infinite waveguides may be questionable. As a consequence, finite-size effects such as a sensitive dependence of the conductivity of finite waveguides on their length, require new theoretical developments and may have potential applications, as discussed below. These results are also relevant for the theory of classical microwave cavities or resonators.

The paper is organized as follows. In Section 2, we adapt the method by Bonnet-Ben Dhia and Joly [27] in order to reduce the original eigenvalue problem in the whole domain to the nonlinear eigenvalue problem in the domain without branches. Although the new problem is more sophisticated, its variational reformulation provides a general framework for proving the trapping (or localization) of eigenfunctions. We use it to derive the main result of the paper: a sufficient condition (18) on the branch lengths for getting a trapped mode. In sharp contrast to infinite non-straight waveguides of a constant cross-section, for which the first eigenfunction is always trapped and exponentially decaying [19], finite waveguides may *or may not* have such an eigenfunction, depending on the length of branches. This method is then illustrated in Section 3 for several finite waveguides (e.g., a bent strip and a cross of two strips). For these examples, we estimate the minimal branch length which is sufficient for getting at least one localized mode. At the same time, we provide an example of a waveguide, for which there is no localization for any branch length. We also construct a family of finite waveguides for which the minimal branch length varies continuously. As a consequence, for a given (large enough) branch length, one can construct two almost identical resonators, one with and the other without localized mode. This observation may be used for developing quantum switching devices.

2 Theoretical results

For the sake of clarity, we start with planar bounded domains with rectangular branches, while the extension to arbitrary domains in $\mathbb{R}^n$ with general cylindrical branches is straightforward and provided at the end of this Section.

We consider a planar bounded domain D composed of a "basic" domain Ω of arbitrary shape and M rectangular branches Q_i of lengths a_i and width b as shown in Figure 1:

$$D = \Omega \cup \bigcup_{i=1}^{M} Q_i.$$

We denote $\Gamma_i = \partial\Omega \cap \partial Q_i$ the inner boundary between the basic domain Ω and the branch Q_i and $\Gamma = \partial\Omega \backslash \bigcup_{i=1}^{M} \Gamma_i$ the exterior boundary of Ω. We study the eigenvalue problem for the Laplace operator with Dirichlet boundary condition

$$-\Delta U = \lambda U, \quad U|_{\partial D} = 0. \tag{1}$$

2.1 Solution in rectangular branches

Let $u_i(x,y)$ denote the restriction of the solution $U(x,y)$ of the eigenvalue problem (1) to the branch Q_i. For convenience, we take $b = 1$ and assume that the coordinates x and y are chosen in such a way that $Q_i = \{(x,y) \in \mathbb{R}^2 \ : \ 0 < x < a_i, \ 0 < y < 1\}$ (the final result will not depend on this particular coordinate system). The eigenfunction $u_i(x,y)$ satisfying Dirichlet boundary condition on ∂Q_i has the standard representation:

$$u_i(x,y) \equiv U_{|Q_i} = \sum_{n=1}^{\infty} c_n \sinh(\gamma_n(a_i - x)) \sin(\pi n y), \tag{2}$$

where $\gamma_n = \sqrt{\pi^2 n^2 - \lambda}$ and c_n are the Fourier coefficients of the function U at the inner boundary Γ_i (at $x = 0$):

$$c_n = \frac{2}{\sinh(\gamma_n a_i)} \int\limits_0^1 dy \; U(0,y) \sin(\pi n y). \tag{3}$$

Substituting this relation into equation (2) yields

$$u_i(x,y) = 2\sum_{n=1}^{\infty} \bigl(U_{|\Gamma_i}, \sin(\pi n y)\bigr)_{L_2(\Gamma_i)} \times \frac{\sinh(\gamma_n(a_i - x))}{\sinh(\gamma_n a_i)} \sin(\pi n y), \tag{4}$$

where the integral in equation (3) was interpreted as the scalar product in $L_2(\Gamma_i)$. The representation (4) is of course formal because its coefficients are still unknown. Nevertheless, one can already distinguish two different cases.

(i) If $\lambda < \pi^2$, all γ_n are real, and the representation (4) decays exponentially. In fact, writing the squared L_2-norm of the function $u_i(x,y)$ along the vertical cross-section of the branch Q_i at x,

$$I_i(x) \equiv \int\limits_0^1 u_i^2(x,y)dy = 2\sum_{n=1}^{\infty} \bigl(U_{|\Gamma_i}, \sin(\pi n y)\bigr)^2_{L_2(\Gamma_i)} \frac{\sinh^2(\gamma_n(a_i - x))}{\sinh^2(\gamma_n a_i)},$$

one uses the inequality $\sinh(\gamma_n(a_i - x)) \leq \sinh(\gamma_n a_i) e^{-\gamma_1 x}$ to get for $0 < x < a_i$

$$I_i(x) \leq 2\sum_{n=1}^{\infty} \bigl(U_{|\Gamma_i}, \sin(\pi n y)\bigr)^2_{L_2(\Gamma_i)} e^{-2\gamma_1 x} = I_i(0) e^{-2\gamma_1 x}. \tag{5}$$

This shows the exponential decay of the eigenfunction along the branch with the decay rate $2\gamma_1 = 2\sqrt{\pi^2 - \lambda}$.

(ii) In turn, if $\lambda > \pi^2$, some γ_n are purely imaginary so that $\sinh(\gamma_n z)$ becomes $\sin(|\gamma_n| z)$, and the exponential decay is replaced by an oscillating behavior. At the same time, this argument does not prohibit the existence of exponentially decaying eigenfunctions with $\lambda > \pi^2$. For an unbounded domain, such eigenfunctions would correspond to the eigenvalues embedded into the continuous spectrum. The detection of such eigenvalues is in general a difficult problem. In this paper, we focus on the isolated eigenvalues below the continuous spectrum (π^2/b^2 for a rectangular branch of width b). It is worth noting that the threshold value π^2/b^2 is the same for finite and infinite waveguides. In what follows, we establish a sufficient condition for getting $\lambda < \pi^2$ that implies the exponential decay of the corresponding eigenfunction according to equation (5).

2.2 Nonlinear eigenvalue problem

The explicit representation (4) of the eigenfunction in the branch Q_i allows one to reformulate the original eigenvalue problem (1) in the whole domain D as a specific eigenvalue problem in the basic domain Ω. In fact, the restriction of U onto the basic domain Ω, $u \equiv U_{|\Omega}$, satisfies the following equations

$$-\Delta u = \lambda u \quad \text{in } \Omega, \qquad u|_{\Gamma} = 0,$$
$$u|_{\Gamma_i} = u_i|_{\Gamma_i}, \qquad \frac{\partial u}{\partial n}|_{\Gamma_i} = -\frac{\partial u_i}{\partial n}|_{\Gamma_i}, \tag{6}$$

where $\partial/\partial n$ denotes the normal derivative directed outwards the domain. The last two conditions ensure that the eigenfunction and its derivative are continuous at inner boundaries Γ_i (the sign minus accounting for opposite orientations of the normal derivatives on both sides of the inner boundary). The normal derivative of u_i can be explicitly written by using equation (4):

$$\begin{aligned}\frac{\partial u_i}{\partial n}|_{\Gamma_i} &= -\frac{\partial u_i}{\partial x}|_{x=0} \\ &= 2\sum_{n=1}^{\infty} \gamma_n \coth(\gamma_n a_i)\big(U_{|\Gamma_i}, \sin(\pi n y)\big)_{L_2(\Gamma_i)} \\ &\quad \times \sin(\pi n y). \end{aligned} \qquad (7)$$

If one denotes $T_i(\lambda)$ an operator acting from $H^{1/2}(\Gamma_i)$ to $H^{-1/2}(\Gamma_i)$ (see [33] for details) as

$$T_i(\lambda) f \equiv 2\sum_{n=1}^{\infty} \gamma_n \coth(\gamma_n a_i)\big(f, \sin(\pi n y)\big)_{L_2(\Gamma_i)} \sin(\pi n y),$$

the right-hand side of equation (7) can be written as

$$\frac{\partial u_i}{\partial n}|_{\Gamma_i} = T_i(\lambda) U_{|\Gamma_i}.$$

The eigenvalue problem (6) admits thus a closed representation as

$$-\Delta u = \lambda u \quad \text{in } \Omega, \quad u|_{\Gamma} = 0, \quad \frac{\partial u}{\partial n}|_{\Gamma_i} = -T_i(\lambda) u|_{\Gamma_i}. \quad (8)$$

The presence of branches and their shapes are fully accounted for by the operators T_i which are somewhat analogous to Dirichlet-to-Neumann operators.

Although this domain decomposition allows one to remove the branches and get a closed formulation for the basic domain Ω, the new eigenvalue problem is *nonlinear* because the eigenvalue λ appears also in the boundary condition through the operators $T_i(\lambda)$. A standard trick to overcome this difficulty goes back to the Birman-Schwinger method [34,35]. Following [27], we fix λ and solve the *linear* eigenvalue problem

$$-\Delta u = \mu(\lambda) u \quad \text{in } \Omega, \quad u|_{\Gamma} = 0, \quad \frac{\partial u}{\partial n}|_{\Gamma_i} = -T_i(\lambda) u|_{\Gamma_i}, \qquad (9)$$

where $\mu(\lambda)$ denotes the eigenvalue which is parameterized by λ. The solution of the original problem is recovered when $\mu(\lambda) = \lambda$.

From a practical point of view, a numerical solution of equations (9) with the subsequent resolution of the equation $\mu(\lambda) = \lambda$ is in general much more difficult than solving the original eigenvalue problem. In turn, equations (9) are convenient for checking whether the eigenvalue λ is smaller or greater than π^2, as explained below.

2.3 Variational formulation

We search for a weak solution of the eigenvalue problem (9) in the space V of functions from the standard Sobolev space $H_0^1(D)$ that are restricted to the basic domain Ω. Multiplying equation (9) by a trial function $v \in V$ and integrating by parts, one gets

$$\mu(\lambda) \int_{\Omega} vu = -\int_{\Omega} v\Delta u = \int_{\Omega} (\nabla v, \nabla u) - \int_{\partial\Omega} v \frac{\partial u}{\partial n}.$$

Since v vanishes on Γ, the weak formulation of the problem reads as

$$(\nabla u, \nabla v)_{L_2(\Omega)} + \sum_{i=1}^{M} \big(T_i(\lambda) u, v\big)_{L_2(\Gamma_i)} = \mu(\lambda) \big(u, v\big)_{L_2(\Omega)}$$

for any trial function $v \in V$. Introducing the Rayleigh's quotient

$$\mu(v;\lambda) = \frac{(\nabla v, \nabla v)_{L_2(\Omega)} + \sum_{i=1}^{M} \big(T_i(\lambda) v, v\big)_{L_2(\Gamma_i)}}{(v,v)_{L_2(\Omega)}}, \quad (10)$$

the first eigenvalue $\mu_1(\lambda)$ is obtained from the Rayleigh's principle

$$\mu_1(\lambda) = \inf_{v\in V,\ v\neq 0} \mu(v;\lambda), \qquad (11)$$

while the other eigenvalues $\mu_k(\lambda)$ $(k = 2, 3, \ldots)$ are determined by the standard minimax description:

$$\mu_k(\lambda) = \sup_{v_1,\ldots,v_{k-1}\in V} \ \inf_{\substack{v\in V,\ v\neq 0,\\ v\perp\{v_1,\ldots,v_{k-1}\}}} \mu(v;\lambda), \qquad (12)$$

where the supremum is taken over $k-1$ linearly independent functions $v_1, \ldots, v_{k-1}$, and the infimum is over functions $v \neq 0$ that are orthogonal to the linear span over $v_1, \ldots, v_{k-1}$.

One can show that $\mu_k(\lambda)$ $(k = 1, 2, 3, \ldots)$ are positive continuous monotonously decreasing functions of λ on the segment $(0, \pi^2]$. For this purpose, one first computes explicitly the derivative of the function

$$h(\lambda) \equiv \gamma_n \coth(\gamma_n a_i) = \sqrt{\pi^2 n^2 - \lambda}\, \coth\left(\sqrt{\pi^2 n^2 - \lambda}\ a_i\right)$$

and checks that $h'(\lambda) < 0$. This implies that $\mu(v,\lambda)$ monotonously decreases with λ for any $v \in V$. Now one can show that $\mu_k(\lambda_1) \leq \mu_k(\lambda_2)$ if $\lambda_1 > \lambda_2$. If some trial functions $v_1, \ldots, v_{k-1} \in V$ and $v \in V$ orthogonal to the linear span $\{v_1, \ldots, v_{k-1}\}$ optimize $\mu(v, \lambda_2)$, one has

$$\mu_k(\lambda_1) \leq \mu(v,\lambda_1) \leq \mu(v,\lambda_2) = \mu_k(\lambda_2),$$

where the monotonous decrease of $\mu(v,\lambda)$ was used (the mathematical proof of the continuity for an analogous functional is given in [36]).

Since the function $\mu_k(\lambda)$ is positive, continuous and monotonously decreasing, the equation $\mu_k(\lambda) = \lambda$ has a solution $0 < \lambda < \pi^2$ if and only if $\mu_k(\pi^2) < \pi^2$. This solution gives the k-th eigenvalue λ_k of the original eigenvalue problem. In what follows, we focus on the first eigenvalue.

2.4 Sufficient condition

Since $\gamma_n(\pi^2) = \pi\sqrt{n^2-1}$, one has $\gamma_1(\pi^2) = 0$, and the operators $T_i(\pi^2)$ can be decomposed into two parts so that the functional $\mu(v) \equiv \mu(v, \pi^2)$ reads

$$\mu(v) = (v,v)^{-1}_{L_2(\Omega)} \Big\{ (\nabla v, \nabla v)_{L_2(\Omega)} + 2\sum_{i=1}^{M} \frac{1}{a_i} (v, \sin(\pi y))^2_{L_2(\Gamma_i)} + 2\pi \sum_{n=2}^{\infty} \sqrt{n^2-1} \sum_{i=1}^{M} \coth\left(\pi a_i \sqrt{n^2-1}\right) \times (v, \sin(\pi n y))^2_{L_2(\Gamma_i)} \Big\}.$$

If one finds a trial function $v \in V$ for which $\mu(v) < \pi^2$, then the first eigenvalue $\mu_1(\pi^2)$ necessarily satisfies this condition because $\mu_1(\pi^2) \leq \mu(v)$. The inequality $\mu(v) < \pi^2$ is thus a sufficient (but not necessary) condition. Given that $\coth(\pi a_i \sqrt{n^2-1}) \leq \coth(\pi a_i \sqrt{3})$ for any $n \geq 2$, the sufficient condition can be written as

$$\sum_{i=1}^{M} \frac{\sigma_i}{a_i} < \beta - \sum_{i=1}^{M} \kappa_i \coth(\pi a_i \sqrt{3}), \tag{13}$$

where

$$\beta = \pi^2 (v,v)_{L_2(\Omega)} - (\nabla v, \nabla v)_{L_2(\Omega)}, \tag{14}$$

$$\sigma_i = 2(v, \sin(\pi y))^2_{L_2(\Gamma_i)}, \tag{15}$$

$$\kappa_i = 2\pi \sum_{n=2}^{\infty} \sqrt{n^2-1}\ (v, \sin(\pi n y))^2_{L_2(\Gamma_i)}. \tag{16}$$

Before presenting examples, several remarks are in order.

(i) The shape of the branches enters through the operators $T_i(\lambda)$. Although the above analysis was presented for rectangular branches, its extension to bounded domains in $\mathbb{R}^n$ with general cylindrical branches is straightforward and based on the variable separation (in directions parallel and perpendicular to the branch). In fact, the Fourier coefficients $(u, \sin(\pi n y))_{L_2(\Gamma_i)}$ on the unit interval (i.e., the cross-section of the rectangular branch) have to be replaced by a spectral decomposition over the orthonormal eigenfunctions $\{\psi_n(y)\}_{n=1}^{\infty}$ of the Laplace operator $\Delta_\perp$ in the cross-section Γ_i of the studied branch (in general, Γ_i is a bounded domain in $\mathbb{R}^{n-1}$):

$$\Delta_\perp \psi_n + \nu_n \psi_n = 0 \quad \text{in } \Gamma_i, \qquad \psi_n|_{\partial\Gamma_i} = 0. \tag{17}$$

In particular, the operator $T_i(\lambda)$ becomes

$$T_i(\lambda) f = \sum_{n=1}^{\infty} \gamma_n \coth(\gamma_n a_i) (f, \psi_n)_{L_2(\Gamma_i)} \psi_n(y),$$

with $\gamma_n = \sqrt{\nu_n - \lambda}$. Repeating the above analysis, one immediately deduces a sufficient condition for getting a trapped mode:

$$\sum_{i=1}^{M} \frac{\sigma_i}{a_i} < \beta - \sum_{i=1}^{M} \kappa_i \coth(a_i \sqrt{\nu_2 - \nu_1}), \tag{18}$$

with

$$\beta = \nu_1 (v,v)_{L_2(\Omega)} - (\nabla v, \nabla v)_{L_2(\Omega)}, \tag{19}$$

$$\sigma_i = (v, \psi_1)^2_{L_2(\Gamma_i)}, \tag{20}$$

$$\kappa_i = \sum_{n=2}^{\infty} \sqrt{\nu_n - \nu_1}\ (v, \psi_n)^2_{L_2(\Gamma_i)}. \tag{21}$$

One retrieves the above results for rectangular branches by putting $\psi_n(y) = \sqrt{2}\sin(\pi n y)$ and $\nu_n = \pi^2 n^2$.

The inequality (18) is the main result of the paper. Although there is no explicit recipe for choosing the trial function v (which determines the coefficients β, σ_i and κ_i), this is a general framework for studying the localization (or trapping) in domains with cylindrical branches.

Since $\sigma_i \geq 0$ and $a_i \geq 0$, the inequality (18) can be satisfied only if the right-hand side is positive. In particular, β should be positive (as both κ_i and $\coth(a_i\sqrt{\nu_2 - \nu_1})$ are positive). The positivity of β is the simplest condition to be checked for choosing the trial function v.

(ii) If the branches are long enough (i.e., $a_i \gg (\nu_2 - \nu_1)^{-1/2}$), the values $\coth(a_i\sqrt{\nu_2-\nu_1})$ are very close to 1 and can be replaced by $1+\epsilon$ where ϵ is set by the expected minimal length so that the inequality (18) becomes more explicit in terms of a_i:

$$\sum_{i=1}^{M} \frac{\sigma_i}{a_i} < \beta - (1+\epsilon) \sum_{i=1}^{M} \kappa_i. \tag{22}$$

In the particular case when all σ_i are the same, one can introduce the threshold value η as

$$\sum_{i=1}^{M} \frac{1}{a_i} < \eta, \qquad \eta \equiv \frac{\beta}{\sigma_1} - \frac{(1+\epsilon)}{\sigma_1} \sum_{i=1}^{M} \kappa_i. \tag{23}$$

For domains with identical branches, $a_i = a$, the above condition determines the branch length $a_{\rm th} = M/\eta$ which is long enough for the emergence of localization. When $\eta > 0$ and $a > a_{\rm th}$, there is a localized eigenmode. Since $a_{\rm th}$ was obtained from the sufficient condition (18), the opposite statement is not true: for $a < a_{\rm th}$, this condition does not indicate whether the eigenfunction is localized or not. In fact, $a_{\rm th}$ is an upper bound for the minimal branch length $a_{\rm min}$ which may distinguish waveguides with and without localized modes (see Sect. 3).

(iii) The trial function should be chosen to ensure the convergence of the series in equation (21). If the boundary of Ω is smooth, the series in equation (21) converges for any function v from V according to the trace theorem [33]. In turn, the presence of corners or other singularities may require additional verifications for the convergence, as illustrated in Section 3.3.

(iv) The implementation of various widths b_i of the rectangular branches is straightforward (e.g., $\sin(\pi ny)$ is replaced by $\sin(\pi ny/b_i)$, etc.). In order to guarantee the exponential decay in all branches, one needs $\lambda < \pi^2/b_i^2$ for all i, i.e., $\lambda < \pi^2/\max\{b_i^2\}$. Rescaling the whole domain in such a way that $\max\{b_i\} = 1$, one can use the above conditions.

(v) The estimate $\mu(v)$ is not an upper bound for the eigenvalue λ. On one hand, one has $\lambda = \mu_1(\lambda) \geq \mu_1(\pi^2)$ because the function $\mu_1(\lambda)$ is monotonously decreasing. On the other hand, $\mu(v) \geq \mu_1(\pi^2)$ according to the definition of $\mu_1(\pi^2)$ as the infimum of the functional $\mu(v)$. As a consequence, λ can be larger or smaller than $\mu(v)$. In turn, the inequality $\mu(v) < \pi^2$ implies $\mu_1(\pi^2) < \pi^2$ which in turn implies $\lambda < \pi^2$ and ensures the localization of the corresponding eigenfunction.

(vi) The above analysis was focused on the first eigenvalue. In particular, the sufficient condition (18) ensures that the first eigenmode is localized. At the same time, the examples of waveguides with numerous localized states were reported in the literature. For instance, Avishai et al. demonstrated the existence of many localized states for a sharp "broken strip", i.e. a waveguide made of two channels of equal width intersecting at a small angle θ [37]. Carini and co-workers reported an experimental confirmation of this prediction and its further extensions [4,6]. Bulgakov et al. considered two straight strips of the same width which cross at an angle $\theta \in (0, \pi/2)$ and showed that, for small θ, the number of localized states is greater than $(1 - 2^{-2/3})^{3/2}/\theta$ [38]. Even for the simple case of two strips crossed at the right angle $\theta = \pi/2$, Schult et al. showed the existence of two localized states, one lying below the cut-off frequency and the other being embedded into the continuous spectrum [2]. The latter state is localized only because it has odd parity with respect to the fourfold rotational symmetry of this waveguide. The above variational approach allows one to investigate the localization of the second and higher-order eigenfunctions that correspond to isolated eigenvalues lying below the continuous spectrum (here, $\lambda_k < \pi^2$). While this is an interesting perspective for future work, we keep considering the first eigenvalue in the following examples.

3 Several examples

As we already mentioned, there is no general recipe for choosing a trial function v. Of course, the best possible choice is the eigenfunction on which $\mu(v)$ reaches its minimum. Except for few cases, the eigenfunction is not known but one can often guess how it behaves for a given basic domain. Since the gradient of the trial function v enters into the coefficient β with the sign minus, slowly varying functions are preferred. In what follows, we illustrate these concepts for several examples.

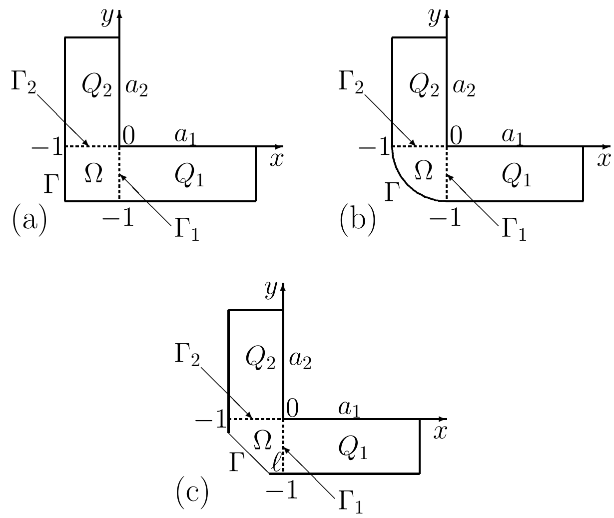

Fig. 2. Three types of a bent waveguide: (a) L-shape, (b) bent strip, and (c) truncated L-shapes parameterized by the length ℓ varying from 0 (triangular basic domain) to 1 (the original L-shape).

3.1 L-shape

We start by a classical problem of localization in L-shape with two rectangular branches of lengths a_1 and a_2 (Fig. 2a) for which the basic domain is simply the unit square. In the limit case $a_1 = a_2 = 0$ (i.e., $D = \Omega$, without branches), the first eigenvalue $\lambda_1 = 2\pi^2 > \pi^2$ so that, according to our terminology, there is no localization. Since λ_1 continuously varies with a ($a_1 = a_2 = a$), the inequality $\lambda_1 > \pi^2$ also remains true for relatively short branches. In turn, given that $\lambda_1 < \pi^2$ for infinitely long branches, there should exist the minimal branch length $a_{\min}$ such that $\lambda_1 = \pi^2$. At this length, the first eigenfunction passes from non-localized state ($a < a_{\min}$) to localized state ($a > a_{\min}$). In what follows, we employ the sufficient condition (13) in order to get an upper bound for $a_{\min}$.

The most intuitive choice for the trial function would be the first eigenfunction for the unit square with Dirichlet boundary condition, $v(x, y) = \sin(\pi x)\sin(\pi y)$. However, one easily checks that $\beta = 0$ for this function, while σ_i and κ_i are always non-negative. As a consequence, the condition (13) is never satisfied for this trial function. It simply means that the first choice was wrong.

For the trial function

$$v(x, y) = (1 + x)\sin(\pi y) + (1 + y)\sin(\pi x), \qquad (24)$$

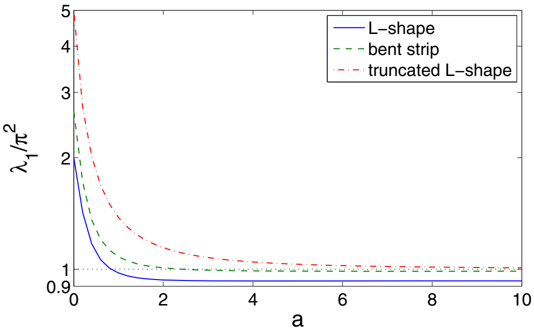

Fig. 3. (Color online) The first eigenvalue λ_1 divided by π^2, as a function of the branch length a ($a_1 = a_2 = a$), for three bent waveguides shown in Figure 2: L-shape (solid line), bent strip (dashed line) and truncated L-shape with $\ell = 0$ (dash-dotted line). For the first two cases, the curves cross the level 1 at $a_{\min} \approx 0.84$ and $a_{\min} \approx 2.44$, respectively. In turn, the third curve always remains greater than 1 (see explanations in Sect. 3.4). For $a = 0$, λ_1 is respectively equal to $2\pi^2$, $4j_{0,1}^2$ and $5\pi^2$, where $j_{0,1} \approx 2.4048$ is the first positive zero of the Bessel function $J_0(z)$.

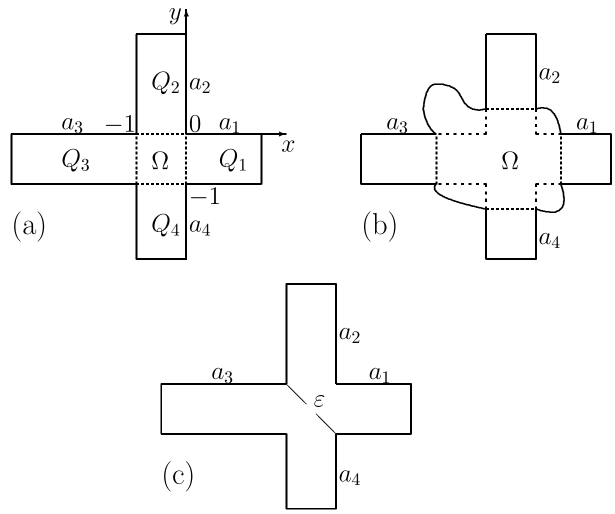

Fig. 4. (a) Crossing of two rectangular branches; (b) an extension of the related basic domain Ω; and (c) coupling between two waveguides from Figure 2c ($\ell = 0$) with an opening of size ε.

the explicit integration yields

$$\beta = 1, \quad \sigma_1 = \sigma_2 = \frac{1}{2}, \quad \kappa_1 = \kappa_2 = 0.$$

The condition (13) reads as

$$\frac{1}{a_1} + \frac{1}{a_2} < 2. \tag{25}$$

If the branches have the same length, $a_1 = a_2 = a$, then the upper bound of the minimal branch length for getting a localized eigenfunction is given by $a_{\text{th}} = 1$.

We also solved the original eigenvalue problem (1) for L-shape with $a_1 = a_2 = a$ by a finite element method (FEM) implemented in Matlab PDEtools. The first eigenvalue λ_1 as a function of the branch length a is shown by solid line in Figure 3. One can clearly see a transition from non-localized ($\lambda_1 > \pi^2$) to localized ($\lambda_1 < \pi^2$) states when a crosses the minimal branch length $a_{\min} \approx 0.84$. As expected, the theoretical upper bound a_{th} which was obtained from a *sufficient* condition, exceeds the numerical value $a_{\min}$. In order to improve the theoretical estimate, one has to search for trial functions which are closer to the true eigenfunction. At the same time, a_{th} and $a_{\min}$ are close to each other, and the accuracy of the theoretical result is judged as good. Similar results for L-shape in three dimensions are derived in Appendix A.

3.2 Cross

Another example is a crossing of two perpendicular rectangular branches (Fig. 4a), for which the basic domain is again the unit square. Since the trial function (24) also satisfies the boundary condition for this problem, the previous sufficient condition (25) remains applicable for arbitrary lengths a_3 and a_4. This is not surprising because any increase of the basic domain decreases the eigenvalue (i.e., if the basic domain was considered as the unit square with two branches Q_3 and Q_4). A symmetry argument implies that other consecutive pairs of branch lengths can be used in the condition (25), e.g., the eigenfunction is localized if $1/a_2 + 1/a_3 < 2$ for arbitrary a_1 and a_4. In turn, the condition $1/a_1 + 1/a_3 < 2$ is not sufficient for localization (in fact, taking $a_2 = a_4 = 0$ yields a rectangle without localization).

The specific feature of the cross is that the exterior boundary of the basic domain Ω consists of 4 corner points. We suggest another trial function

$$v(x, y) = x(1 + x) + y(1 + y), \tag{26}$$

which satisfies the Dirichlet boundary condition at these points. The direct integration yields

$$\beta = \frac{11}{90}\pi^2 - \frac{2}{3}, \qquad \sigma_i = \frac{32}{\pi^6},$$
$$\kappa_i = 2\pi \sum_{n=2}^{\infty} \sqrt{n^2 - 1} \left(2\frac{1 - (-1)^n}{\pi^3 n^3} \right)^2 \approx 4.4768 \times 10^{-4}.$$

The condition (13) reads now as

$$\sum_{i=1}^{4} \frac{1}{a_i} < \frac{\beta}{\sigma_1} - \frac{\kappa_1}{\sigma_1} \sum_{i=1}^{4} \coth\left(\pi a_i \sqrt{3}\right). \tag{27}$$

If all the branches have the same length a, the upper bound of the minimal branch length can be estimated by solving the equation

$$\frac{4}{a_{\text{th}}} = \frac{\beta}{\sigma_1} - \frac{4\kappa_1}{\sigma_1} \coth\left(\pi a_{\text{th}} \sqrt{3}\right),$$

from which one gets $a_{\text{th}} \approx 0.2458$. Note that this result proves and further extends the prediction of localized

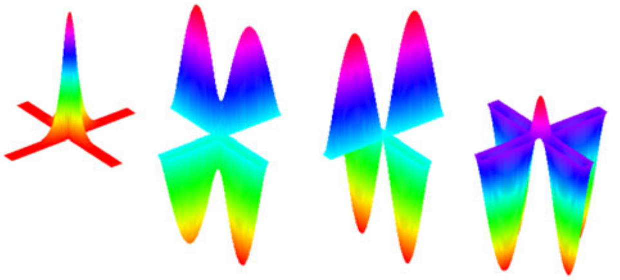

Fig. 5. (Color online) First eigenfunctions for the crossing of two rectangular branches ($a_i = 5$). The associated eigenvalues are $\lambda_1 \approx 0.661\pi^2$, $\lambda_2 = \lambda_3 \approx 1.032\pi^2$, $\lambda_4 \approx 1.036\pi^2$ and $\lambda_5 \approx 1.044\pi^2$.

eigenmodes in the crossing of infinite rectangular strips which was made by Schult et al. by numerical computation [2]. In that reference, the importance of localized electron eigenstates in four terminal junctions of quantum wires was discussed.

We also mention that Freitas and Krejčiřík derived a rigorous upper bound for the first eigenvalue of the Laplace operator in a bounded strictly star-shaped domain in $\mathbb{R}^n$ with locally Lipschitz boundary [39]. In particular, they obtained an explicit formula for the cross with equal branches which reads in our notations as

$$\lambda \le 4j_{0,1}^2 \frac{1 + 2a + 4a^2}{1 + 6a + 8a^2},$$

where $j_{0,1} \approx 2.4048$ is the first zero of the Bessel function $J_0(z)$. However, this upper bound is always greater than π^2 and thus insufficient for determining the localization character of the first eigenfunction.

Figure 5 presents first eigenfunctions for the crossing of two rectangular branches with $a_i = 5$ (the second eigenfunction, which looks similar to the third one, is not shown). As predicted by the sufficient condition (27), the first eigenfunction (with $\lambda_1 \approx 0.66\pi^2$) is clearly localized in the basic domain and exponentially decaying in the branches. In turn, the other eigenfunctions (with $\lambda_n > \pi^2$) presented in Figure 5, are not localized.

It is worth noting again that any increase of the basic domain (see Fig. 4b) reduces the eigenvalue and thus favors the localization.

3.3 Bent strip

In previous examples, the basic domain was the unit square. We consider another shape for which the analytical estimates can be significantly advanced. This is a sector of the unit disk which can be seen as a connector between two parts of a bent strip (Fig. 2b). In contrast to the case of infinite strips for which Goldstone and Jaffe have proved the existence of a localized eigenmode for any bending (except the straight strip) [19], there is a minimal branch length required for the existence of a localized eigenmode in a finite bent strip. In order to demonstrate this result,

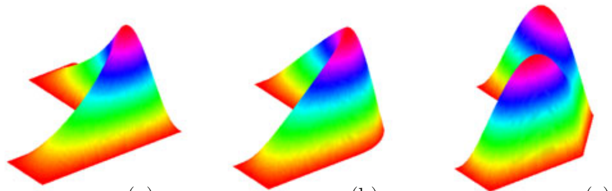

Fig. 6. (Color online) The first eigenfunction for three bent waveguides shown in Figure 2 ($\ell = 0$), with $a = 2$. The associate eigenvalue λ_1 is equal to $0.9357\pi^2$, $1.0086\pi^2$ and $1.1435\pi^2$, respectively. Although the first eigenmode is localized, all three eigenfunctions visually look similar.

we consider the family of trial functions

$$v_\alpha(r) = \frac{\sin \pi r}{r^\alpha} \qquad (0 < \alpha < 1). \tag{28}$$

In Appendix B, we derive equations (B.1)–(B.3) for the coefficients β, σ_i, and κ_i, respectively. Since all these coefficients depend on α, its variation can be used to maximize the threshold η given by equation (23). The numerical computation of these coefficients suggests that η is maximized for α around 1/3: $\eta \approx 0.7154$. If $a_1 = a_2 = a$, one gets an upper bound $a_{\rm th}$ of the minimal branch length which ensures the emergence of the localized eigenfunction:

$$a > a_{\rm th} = \frac{2}{\eta} \approx 2.7956.$$

We remind that this is sufficient, not necessary condition. The numerical computation of the first eigenvalue in the bent strip (by FEM implemented in Matlab PDEtools) yields $a_{\min} \approx 2.44$. One can see that the upper bound $a_{\rm th}$ is relatively close to this value. The behavior of the eigenvalue λ_1 as a function of the branch length a is shown by dashed line in Figure 3.

3.4 Waveguide without localization

Any increase of the basic domain Ω reduces the eigenvalues and thus preserves the localization. In turn, a decrease of Ω may suppress the trapped mode. For instance, the passage from L-shape (Ω being the unit square) to the bent strip (Ω being the quarter of the disk) led to larger minimal length required for keeping the localization ($a_{\min} \approx 2.44$ instead of $a_{\min} \approx 0.84$). For instance, when $a_1 = a_2 = 2$, the first eigenfunction, which was localized in the L-shape, is not localized in the bent strip (Fig. 6). Further decrease of the basic domain Ω may completely suppress the localization.

In order to illustrate this point, we consider the truncated L-shape shown in Figure 2c with $\ell = 0$ for which

$$\Omega = \{(x, y) \in \mathbb{R}^2 \;:\; -1 < x < 0,\; -1 < y < 0,\; x+y > -1\}$$

is a triangle. It is easy to see that $u(x, y) = \cos(\pi x) + \cos(\pi y)$ is the first eigenfunction of the following eigenvalue problem in Ω:

$$-\Delta u = \tilde{\mu} u \quad \text{in } \Omega, \qquad u|_\Gamma = 0, \qquad \frac{\partial u}{\partial n}|_{\Gamma_i} = 0,$$

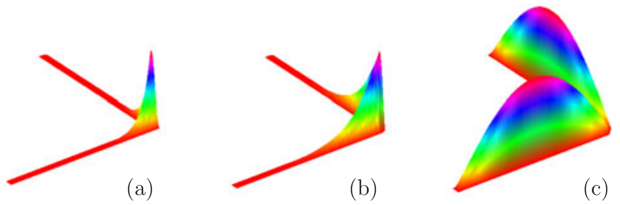

Fig. 7. (Color online) The first eigenfunction for three bent waveguides shown in Figure 2 ($\ell = 0$), with $a = 20$. The associate eigenvalue λ_1 is equal to $0.9302\pi^2$, $0.9879\pi^2$ and $1.0032\pi^2$, respectively. Although the last two values are very close to each other, the behavior of the eigenfunctions is completely different.

with the eigenvalue $\tilde{\mu}_1 = \pi^2$. From the variational principle

$$\tilde{\mu}_1 = \inf_{v\in V, v\neq 0} \frac{\left(\nabla v, \nabla v\right)_{L_2(\Omega)}}{\left(v, v\right)_{L_2(\Omega)}},$$

so that

$$\left(\nabla v, \nabla v\right)_{L_2(\Omega)} \geq \tilde{\mu}_1 \left(v, v\right)_{L_2(\Omega)} = \pi^2 \left(v, v\right)_{L_2(\Omega)}$$

for all $v \in V$. Moreover, the Friedrichs-Poincaré inequality in the branches Q_i implies [33]

$$\left(\nabla v, \nabla v\right)_{L_2(Q_i)} \geq \pi^2 \left(v, v\right)_{L_2(Q_i)} \quad \forall v \in H_0^1(Q_i),$$

from which

$$\left(\nabla v, \nabla v\right)_{L_2(D)} \geq \pi^2 \left(v, v\right)_{L_2(D)} \quad \forall v \in H_0^1(D).$$

As a consequence, all eigenvalues of the original eigenvalue problem (1) in D exceed π^2 and the corresponding eigenfunctions are not localized in the basic domain Ω, whatever the length of the branches (note that here $\beta \leq 0$).

When one varies continuously ℓ in Figure 2c, the basic domain transforms from the unit square (Fig. 2a) to the right triangle so that one can get any prescribed minimal length $a_{\min}$ between 0.84 and infinity. In other words, for any prescribed branch length, one can always design such a basic domain (such ℓ) for which there are no localized eigenmodes. As a consequence, the localization may be very sensitive to the shape of the basic domain and to the length of branches. These effects which were overseen for infinite waveguides, may be important for microelectronic applications.

Figure 7 shows the first eigenfunction for three bent waveguides from Figure 2 with $a = 20$. The associate eigenvalue λ_1 is equal to $0.9302\pi^2$, $0.9879\pi^2$ and $1.0032\pi^2$, respectively. Although the last two values are very close to each other, the behavior of the associated eigenfunctions is completely different. According to the sufficient condition, the first two eigenfunctions are localized in the basic domain, while the last one is not. One can clearly distinguish these behaviors in Figure 7.

3.5 Two coupled waveguides

The coupling of infinite waveguides has been intensively investigated [40]. We consider a coupling of two finite crossing waveguides through an opening of variable size ε as shown in Figure 4c. When $\varepsilon = 0$, one has two decoupled waveguides from Figure 2c for which we proved in the previous subsection the absence of localized eigenmodes. When $\varepsilon = \sqrt{2}$, there is no barrier and the waveguides are fully coupled. This is the case of crossing between two rectangular branches as shown in Figure 4a, for which we checked the existence of localized eigenmodes under weak conditions (25) or (27). Varying the opening ε from 0 to $\sqrt{2}$, one can continuously pass from one situation to the other. This transition is illustrated in Figure 8 which presents the first eigenfunction for two coupled waveguides shown in Figure 4c, with $a_i = 5$ and different coupling (opening ε). The first two eigenfunctions, with $\varepsilon = 0$ (fully separated waveguides) and $\varepsilon = 0.4\sqrt{2}$ (opening 40%), are not localized, while the last two eigenfunctions, with $\varepsilon = 0.5\sqrt{2}$ (opening 50%) and $\varepsilon = \sqrt{2}$ (fully coupled waveguides, i.e. a cross), are localized. The critical coupling ε_c, at which the transition occurs (i.e., for which $\lambda_1 = \pi^2$) lies between 40% and 50%. Although numerical computation may allow one to estimate ε_c more accurately, we do not perform this analysis because the value ε_c anyway depends on the branch lengths. In general, for any $a > a_{\min} \approx 0.84$, there is a critical value $\varepsilon_c(a)$ for which $\lambda_1 = \pi^2$. For $\varepsilon < \varepsilon_c$, there is no localized modes, while for $\varepsilon > \varepsilon_c$ there is at least one localized mode. The high sensitivity of the localization character to the opening ε and to the branch lengths can potentially be employed in quantum switching devices (see [1] and references therein).

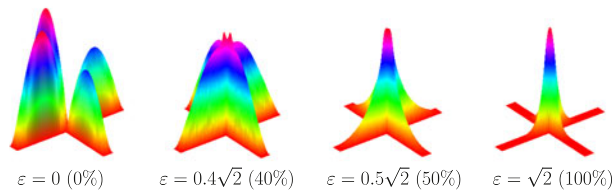

Fig. 8. (Color online) The first eigenfunction for two coupled waveguides shown in Figure 4c, with $a_i = 5$ and different coupling (opening ε): $\varepsilon = 0$ (fully separated waveguides, zero coupling), $\varepsilon = 0.4\sqrt{2}$ (opening 40% of the diagonal), $\varepsilon = 0.5\sqrt{2}$ (opening 50% of the diagonal) and $\varepsilon = \sqrt{2}$ (fully coupled waveguides, no barrier). The associate eigenvalue λ_1 is equal to $1.05\pi^2$, $1.02\pi^2$, $0.97\pi^2$, and $0.67\pi^2$, respectively. In the first two cases, the eigenmodes is not localized. Changing the opening ε, one passes from non-localized to localized eigenmodes.

Conclusion

We investigated the problem of trapped or localized eigenmodes of the Laplace operator in cavities or resonators with long branches that we called "finite waveguides". In this context, the localization was understood as an exponential decay of an eigenfunction inside the branches. This behavior was related to the smallness of the associated eigenvalue λ in comparison to the first eigenvalue of the Laplace operator in the cross-section of the branch with Dirichlet boundary condition. Using the explicit representation of an eigenfunction in branches, we proposed a general variational formalism for checking the existence of localized modes. The main result of the paper is the sufficient condition (18) on the branch lengths for getting a trapped mode. In spite of the generality of the formalism, a practical use of the sufficient condition relies on an intuitive choice of the trial function in the basic domain (without branches). This function should be as close as possible to the (unknown) eigenfunction. Although there is no general recipe for choosing trial functions, one can often guess an appropriate choice, at least for relatively simple domains.

These points were illustrated for several typical waveguides, including 2D and 3D L-shapes, crossing of the rectangular strips, and bent strips. For all these cases, the basic domain was simple enough to guess an appropriate trial function in order to derive an explicit sufficient condition for getting at least one localized mode. In particular, we obtained an upper bound of the minimal branch length which is sufficient for localization. We proved the existence of a trapped mode in finite L-shape, bent strip and cross of two strips provided that their branches are long enough, with an accurate estimate on the required minimal length. These results were confirmed by a direct numerical resolution of the original eigenvalue problem by finite element method implemented in Matlab PDEtools. The presented method can be applied for studying the localization in many other waveguides, e.g. smooth bent strip [10], sharply bent strip [4,37], Z-shapes [5] or two strips crossing at arbitrary angle [38]. The use of our theoretical approach for studying the localization of the second and higher eigenmodes presents an interesting perspective.

It is worth emphasizing that the distinction between localized and non-localized modes is much sharper in infinite waveguides than in finite ones. Although by definition the localized eigenfunction in a finite waveguide decays exponentially, the decay rate may be arbitrarily small. If the branch is not long enough, the localized mode may be visually indistinguishable from a non-localized one, as illustrated in Figure 6. In turn, the distinction between localized and non-localized modes in infinite waveguides is always present, whatever the value of the decay rate.

The main practical result is an explicit construction of two families of waveguides (truncated L-shapes in Fig. 2c and coupled waveguides in Fig. 4c), for which the minimal branch length $a_{\min}$ for getting a trapped mode continuously depends on the parameter ℓ or ε of the basic domain. For any prescribed (long enough) branch length, one can thus construct two almost identical finite waveguides, one with and the other without a trapped mode. The high sensitivity of the localization character to the shape of the basic domain and to the length of branches may potentially be used for switching devices in microelectronics and optics.

This work has been partly supported by the RFBR No. 09-01-00408a grant and the ANR grant “SAMOVAR”.

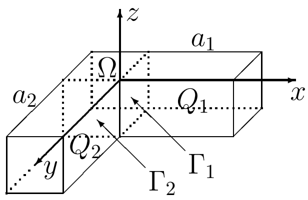

Fig. A.1. L-shape in three dimensions for which the basic domain $\Omega = [-1, 0]^3$ is the unit cube.

Appendix A: L-shape in three dimensions

As we mentioned at the end of Section 2, an extension of the presented approach to other types of branches is straightforward. We illustrate this point by considering the L-shape in three dimensions, i.e. two connected parallelepipeds of cross-section in the form of the unit square, for which the basic domain Ω is the unit cube (Fig. A.1). For each branch, the eigenvalues and eigenfunctions in equation (17) for the cross-section can be parameterized by two indexes m and n:

$$\nu_{m,n} = \pi^2(m^2 + n^2), \quad \psi_{m,n}(y, z) = 2\sin(\pi m y)\sin(\pi n z)$$

(similar for the second branch).

We take the trial function

$$v(x, y, z) = \big[(1 + x)\sin(\pi y) + (1 + y)\sin(\pi x)\big]\sin(\pi z),$$

which satisfies the Dirichlet boundary condition. The coefficients β, σ_i and κ_i can be found from equations (19)–(21), for which the explicit integration yields

$$\big(v, v\big)_{L_2(\Omega)} = \int_{-1}^{0} dx \int_{-1}^{0} dy \int_{-1}^{0} dz\ v^2 = \frac{1}{6} + \frac{1}{\pi^2},$$

$$\big(\nabla v, \nabla v\big)_{L_2(\Omega)} = \int_{-1}^{0} dx \int_{-1}^{0} dy \int_{-1}^{0} dz \big(\nabla v, \nabla v\big) = \frac{\pi^2}{3} + \frac{3}{2},$$

so that $\beta = 2\pi^2\big(\nabla v, \nabla v\big)_{L_2(\Omega)} - \big(v, v\big)_{L_2(\Omega)} = 1/2$, and

$$\big(v, \psi_{1,1}\big)_{L_2(\Gamma_1)} = \int_{-1}^{0} dy \int_{-1}^{0} dz\ v(0, y, z)\, 2\sin(\pi y)\sin(\pi z) = \frac{1}{2},$$

while $\big(v, \psi_{m,n}\big)_{L_2(\Gamma_1)} = 0$ for $m \neq 1$ or $n \neq 1$, from which $\sigma_1 = \sigma_2 = 1/4$ and $\kappa_1 = \kappa_2 = 0$. The condition (18) reads as

$$\frac{1}{a_1} + \frac{1}{a_2} < 2.$$

If the branches have the same length, $a_1 = a_2 = a$, then the upper bound of the minimal branch length for getting a localized eigenfunction is given by $a_{\rm th} = 1$, as in two dimensions.

Appendix B: Computation for bent strip

The computation of the coefficients β and σ_i is straightforward, while that for κ_i requires supplementary estimates.

Coefficient β. One has

$$(v_\alpha, v_\alpha)_{L_2(\Omega)} = \frac{\pi}{2}\int_0^1 r^{1-2\alpha}\sin^2(\pi r)dr = \frac{\pi}{4}\left[\frac{1}{2(1-\alpha)} - w_{2\alpha-1}(2\pi)\right],$$

where

$$w_\nu(q) \equiv \int_0^1 r^{-\nu}\cos(qr)dr.$$

Similarly,

$$(\nabla v_\alpha, \nabla v_\alpha)_{L_2(\Omega)} = \frac{\pi}{2}\int_0^1 r(v'_\alpha)^2 dr = \frac{\pi}{2}\int_0^1 r\left(\frac{\pi\cos\pi r}{r^\alpha} - \frac{\alpha\sin\pi r}{r^{1+\alpha}}\right)^2 dr.$$

Expanding the quadratic polynomial and integrating by parts, one gets

$$(\nabla v_\alpha, \nabla v_\alpha)_{L_2(\Omega)} = \frac{\pi^3}{4}\left[\frac{1}{2(1-\alpha)} + \frac{w_{2\alpha-1}(2\pi)}{1-2\alpha}\right].$$

Combining this term with the previous result yields

$$\beta = \frac{\pi^3}{4}\frac{2\alpha}{2\alpha-1}w_{2\alpha-1}(2\pi). \qquad \text{(B.1)}$$

In the limit $\alpha \to 1/2$, one has

$$\lim_{\alpha\to 1/2}\frac{w_{2\alpha-1}(2\pi)}{2\alpha-1} = \frac{\mathrm{Si}(2\pi)}{2\pi} \approx 0.2257,$$

where $\mathrm{Si}(x)$ is the integral sine function.

Coefficients σ_i. For these coefficients, one gets

$$\big(v_\alpha, \sin(\pi r)\big)_{L_2(\Gamma_i)} = \int_0^1 r^{-\alpha}\sin^2(\pi r)dr = \frac{1}{2}\left(\frac{1}{1-\alpha} - w_\alpha(2\pi)\right),$$

from which

$$\sigma_1 = \sigma_2 = \frac{1}{2}\left(\frac{1}{1-\alpha} - w_\alpha(2\pi)\right)^2. \qquad \text{(B.2)}$$

Coefficients κ_i. One considers

$$\big(v_\alpha, \sin(\pi n r)\big)_{L_2(\Gamma_i)} = \int_0^1 r^{-\alpha}\sin(\pi r)\sin(\pi n r)dr = \frac{1}{2}\Big[w_\alpha(\pi(n-1)) - w_\alpha(\pi(n+1))\Big].$$

The function $w_\alpha(q)$ can be decomposed into two parts [41],

$$w_\alpha(q) = \int_0^\infty r^{-\alpha}\cos(qr)dr - \int_1^\infty r^{-\alpha}\cos(qr)dr = q^{\alpha-1}\frac{\sqrt{\pi}\,\Gamma(\frac{1-\alpha}{2})}{2^\alpha\Gamma(\frac{\alpha}{2})} - \tilde{w}_\alpha(q),$$

where

$$\tilde{w}_\alpha(q) \equiv \int_1^\infty r^{-\alpha}\cos(qr)dr.$$

We have

$$\kappa_i = 2\pi\sum_{n=2}^\infty \sqrt{n^2-1}\,\big(v, \sin(\pi n r)\big)^2_{L_2(\Gamma_i)} = 2\pi\sum_{n=2}^\infty \sqrt{n^2-1}\,(d_n - e_n)^2,$$

where

$$d_n = \frac{\pi^{\alpha-\frac{1}{2}}\,\Gamma(\frac{1-\alpha}{2})}{2^{1+\alpha}\Gamma(\frac{\alpha}{2})}\Big[(n-1)^{\alpha-1} - (n+1)^{\alpha-1}\Big],$$
$$e_n = \frac{1}{2}\Big[\tilde{w}_\alpha(\pi(n-1)) - \tilde{w}_\alpha(\pi(n+1))\Big].$$

In order to estimate the coefficients e_n, the function $\tilde{w}_\alpha(q)$ is integrated by parts that yields for $q = \pi(n \pm 1)$:

$$\tilde{w}_\alpha(q) = \alpha\frac{\cos q}{q^2} - \alpha(\alpha+1)\frac{\tilde{w}_{\alpha+2}(q)}{q^2} = \alpha\frac{\cos q}{q^2} - \alpha(\alpha+1)(\alpha+2)\frac{\cos q}{q^4} + \alpha(\alpha+1)(\alpha+2)(\alpha+3)\frac{\tilde{w}_{\alpha+4}(q)}{q^4}.$$

The inequality

$$(\alpha+3)|\tilde{w}_{\alpha+4}(q)| \le (\alpha+3)\int_1^\infty r^{-\alpha-4}dr = 1$$

leads to

$$\alpha\frac{\cos q}{q^2} - \alpha(\alpha+1)(\alpha+2)\frac{\cos q + 1}{q^4} \le \tilde{w}_\alpha(q) \le \alpha\frac{\cos q}{q^2} - \alpha(\alpha+1)(\alpha+2)\frac{\cos q - 1}{q^4},$$

from which

$$e_n^- \le e_n \le e_n^+,$$

where lower and upper bounds are

$$e_n^\pm = \frac{1}{2}\left[\left(\frac{\alpha}{\pi^2}\frac{(-1)^{n-1}}{(n-1)^2} - \frac{\alpha(\alpha+1)(\alpha+2)}{\pi^4}\frac{(-1)^{n-1}\mp 1}{(n-1)^4}\right) - \left(\frac{\alpha}{\pi^2}\frac{(-1)^{n+1}}{(n+1)^2} - \frac{\alpha(\alpha+1)(\alpha+2)}{\pi^4}\frac{(-1)^{n+1}\pm 1}{(n+1)^4}\right)\right].$$

Using these estimates, one gets

$$\sum_{n=2}^{\infty} \sqrt{n^2-1}\, d_n^2 \equiv A_1,$$
$$\sum_{n=2}^{\infty} \sqrt{n^2-1}\, d_n e_n \geq \sum_{n=2}^{\infty} \sqrt{n^2-1}\, d_n e_n^- \equiv A_2^-,$$
$$\sum_{n=2}^{\infty} \sqrt{n^2-1}\, e_n^2 \leq \sum_{n=2}^{\infty} \sqrt{n^2-1}\, (e_n^+)^2 \equiv A_3^+,$$

from which

$$\kappa_i \leq \kappa, \qquad \kappa \equiv 2\pi(A_1 - 2A_2^- + A_3^+). \tag{B.3}$$

Although the expressions for A_1, A_2^- and A_3^+ are cumbersome, the convergence of these series can be easily checked, while their numerical evaluation is straightforward.

The numerical computation of these coefficients shows that the threshold value η is maximized at $\alpha \approx 1/3$: $\eta \approx 0.7154$. Note that if the coefficients κ_i were computed by direct numerical integration and summation, the value of η for $\alpha = 1/3$ could be slightly improved to be 0.7256. The difference results from the estimates we used, and its smallness indicates that the estimates are quite accurate.

References

1. G. Timp, H.U. Baranger, P. deVegvar, J.E. Cunningham, R.E. Howard, R. Behringer, P.M. Mankiewich, Phys. Rev. Lett. **60**, 2081 (1988)
2. R.L. Schult, D.G. Ravenhall, H.W. Wyld, Phys. Rev. B **39**, 5476 (1989)
3. J.P. Carini, J.T. Londergan, K. Mullen, D.P. Murdock, Phys. Rev. B **46**, 15538 (1992)
4. J.P. Carini, J.T. Londergan, K. Mullen, D.P. Murdock, Phys. Rev. B **48**, 4503 (1993)
5. J.P. Carini, J.T. Londergan, D.P. Murdock, D. Trinkle, C.S. Yung, Phys. Rev. B **55**, 9842 (1997)
6. J.T. Londergan, J.P. Carini, D.P. Murdock, *Binding and Scattering in Two-Dimensional Systems: Applications to Quantum Wires, Waveguides and Photonic Crystals* (Springer, Berlin, 1999)
7. P. Duclos, P. Exner, Rev. Math. Phys. **7**, 73 (1995)
8. J.D. Jackson, *Classical Electrodynamics*, 3rd edn. (Wiley & Sons, New York, 1999)
9. C.M. Linton, P. McIver, Wave Motion **45**, 16 (2007)
10. O. Olendski, L. Mikhailovska, Phys. Rev. E **81**, 036606 (2010)
11. F. Rellich, *Das Eigenwertproblem von in Halbrohren*, (Studies and Essays Presented to R. Courant, New York, 1948), pp. 329–344
12. D.S. Jones, Math. Proc. Camb. Phil. Soc. **49**, 668 (1953)
13. F. Ursell, Math. Proc. Camb. Phil. Soc. **47**, 347 (1951)
14. F. Ursell, J. Fluid Mech. **183**, 421 (1987)
15. F. Ursell, Proc. R. Soc. Lond. A **435**, 575 (1991)
16. R. Parker, J. Sound Vib. **4**, 62 (1966)
17. R. Parker, J. Sound Vib. **5**, 330 (1967)
18. P. Exner, P. Seba, J. Math. Phys. **30**, 2574 (1989)
19. J. Goldstone, R.L. Jaffe, Phys. Rev. B **45**, 14100 (1992)
20. B. Chenaud, P. Duclos, P. Freitas, D. Krejcirík, Diff. Geom. Appl. **23**, 95 (2005)
21. D.V. Evans, IMA J. Appl. Math. **49**, 45 (1992)
22. D.V. Evans, M. Levitin, D. Vassiliev, J. Fluid Mech. **261**, 21 (1994)
23. E.B. Davies, L. Parnovski, Q.J. Mech. Appl. Math. **51**, 477 (1998)
24. W. Bulla, F. Gesztesy, W. Renger, B. Simon, Proc. Amer. Math. Soc. **125**, 1487 (1997)
25. J. Dittrich, J. Kríz, J. Phys. A: Math. Gen. **35**, L269 (2002)
26. P. Freitas, D. Krejčiřík, Math. Phys. Anal. Geom. **9**, 335 (2006)
27. A.S. Bonnet-Ben Dhia, P. Joly, SIAM J. Appl. Math. **53**, 1507 (1993)
28. M.S. Ashbaugh, P. Exner, Phys. Lett. A **150**, 183 (1990)
29. P. Exner, P. Freitas, D. Krejčiřík, Proc. R. Soc. Lond. A **460**, 3457 (2004)
30. B. Sapoval, T. Gobron, A. Margolina, Phys. Rev. Lett. **67**, 2974 (1991)
31. C. Even, S. Russ, V. Repain, P. Pieranski, B. Sapoval, Phys. Rev. Lett. **83**, 726 (1999)
32. S. Felix, M. Asch, M. Filoche, B. Sapoval, J. Sound. Vib. **299**, 965 (2007)
33. J.L. Lions, E. Magenes, *Non-homogeneous Boundary value Problems and Applications* (Springer-Verlag, Berlin, New York, 1972)
34. M.S. Birman, Mat. Sbornik **55**, 125 (1961) [in Russian]
35. J. Schwinger, Proc. Natl. Acad. Sci. **47**, 122 (1961)
36. A.L. Delitsyn, Diff. Equ. **40**, 207 (2004)
37. Y. Avishai, D. Bessis, B.G. Giraud, G. Mantica, Phys. Rev. B **44**, 8028 (1991)
38. E.N. Bulgakov, P. Exner, K.N. Pichugin, A.F. Sadreev, Phys. Rev. B **66**, 155109 (2002)
39. P. Freitas, D. Krejčiřík, Proc. Amer. Math. Soc. **136**, 2997 (2008)
40. P. Exner, P. Seba, M. Tater, D. Vanek, J. Math. Phys. **37**, 4867 (1996)
41. I.S. Gradshteyn, I.M. Ryzhik, *Table of Integrals, Series and Products* (Academic Press, New York, 1980)